

Quantum chaos and pole-skipping in a semilocally critical IR fixed point

Hyun-Sik Jeong *

*Instituto de Física Teórica UAM/CSIC, c/Nicolás Cabrera 13-15,
Universidad Autónoma de Madrid, Cantoblanco, 28049 Madrid, Spain.*

We investigate pole-skipping and its connection with quantum chaos, emphasizing the role of the IR fixed point in the established relationship between pole-skipping and a universal bound of the energy diffusion constant. Using the holographic Gubser-Rocha model, which features a semi-locally critical IR fixed point, we refine the pole-skipping argument to apply to generic fixed points. Additionally, we explore the reconstruction of the full hydrodynamic dispersion relation through pole-skipping. By considering conditions in which the dispersion relation exhibits the energy diffusive mode at low wave-vector and passes through a pole-skipping point, we propose an effective heuristic approximation. This approximation is valid in strong momentum relaxation and relies on three physical quantities: (D_e, v_B, λ_L) , determined from horizon data. Here, D_e represents the energy diffusion constant, v_B the butterfly velocity, and λ_L the Lyapunov exponent. Remarkably, this approximation demonstrates excellent agreement with the quasi-normal mode, even extending its applicability beyond the hydrodynamic regime.

I. INTRODUCTION

Chaos is an ubiquitous phenomenon that arises widely in nature. Whilst significant progress has been made in understanding chaos at the classical level, its characterization and manifestation at the quantum level remain considerably less understood, particularly within the context of many-body systems.

In recent years, there has been notable advancement in the characterization of chaotic behavior within quantum many-body systems, primarily through the utilization of out-of-time ordered correlation functions (OTOCs) [1]. For instance, for chaotic systems, OTOCs can exhibit

$$\langle V(t, x)W(0)V(t, x)W(0) \rangle = 1 - \epsilon e^{\lambda_L(t-|x|/v_B)} + \dots, \quad (1)$$

where V and W represent generic local operators and ϵ is a non-universal component related to the operators involved in OTOCs. The exponential growth in (1) is reminiscent of the divergence of trajectories between two particles that were initially infinitesimally separated in classical chaotic systems. In this regard, λ_L is often referred to as the quantum Lyapunov exponent, and v_B the butterfly velocity.

The quantum nature of (1) can become evident by the upper bound of λ_L as $\lambda_L \leq 2\pi T k_B/\hbar$ [2] (hereafter, we set $k_B = \hbar = 1$). Maximally chaotic systems, those that attain the upper bound, can be achieved in a range of systems, including holographic theories, two-dimensional conformal field theories in the large central charge limit, and strongly coupled SYK models.

At the classical level, chaos is thought to underlie the microscopic dynamic processes governing macroscopic phenomena like transport and thermalization, as demonstrated in prior works [3, 4]. However, it remains an unresolved question whether chaos plays

a similar fundamental role in the context of quantum many-body systems. Encouragingly, there have been several intriguing indications suggesting that equation (1) is intricately linked to transport and hydrodynamic behavior [5–17].

Quantum chaos and pole-skipping. Given that the hydrodynamic degrees of freedom represents a universal sector across various quantum many-body systems, it is inherently reasonable to explore a hydrodynamic origin of the chaotic behavior, e.g., OTOCs. In this context, significant progress has been made, revealing that quantum chaos can also manifest in the thermal energy density two-point functions [12, 13] alongside OTOCs. This characteristic phenomenon is known as “pole-skipping” and was initially observed through numerical investigations in holographic systems [12]. Subsequently, it has been theoretically established as a general prediction within the framework of an effective field theory for maximally chaotic systems [13].

To elaborate further, pole-skipping refers to a specific point in the momentum space where the energy density two-point function becomes ill-defined. This special point is referred to as the pole-skipping point denoted by (ω_*, k_*) :

$$\omega_* = i\lambda_L, \quad k_* = i\frac{\lambda_L}{v_B}. \quad (2)$$

As the line of poles passes through this special point, the theory predicts that the residue of the two-point function should also vanish so that the pole is “skipped”.

The relationship between OTOCs (1) and the pole-skipping point (2) can be elucidated by expressing OTOCs in terms of plane waves, specifically as OTOCs = $1 - \epsilon e^{-i\omega t + ikx} + \dots$ when $(\omega, k) = (\omega_*, k_*)$.

Pole-skipping can also be understood through the properties of black hole horizons in holography. In general, the two-point function is determined by imposing an incoming boundary condition at the horizon. However,

* hyunsik.jeong@csic.es

at the specific point (2), it is found that the outgoing solution can also serve as an incoming solution, leading to the existence of two independent solutions near the horizon, thereby rendering the two-point function non-uniquely defined.

Additionally, apart from the non-uniqueness of incoming solutions, it has also been demonstrated that the pole-skipping point can be identified through the horizon analysis of Einstein’s equations of motion. This method is known as the near-horizon analysis. Pole-skipping has been confirmed in SYK chains [5] and has also been validated in two-dimensional CFTs when the central charge is large [18]. The physical and mathematical nature of the pole-skipping phenomenon has been extensively explored and studied in various scenarios, for instance see [19–47].

In essence, the pole-skipping phenomena not only can serve as a “smoking-gun” for the hydrodynamic origin of the chaotic behavior, but also offers a more straightforward method for computing λ_L and v_B directly from the energy density two-point function, bypassing the need for OTOCs calculations.

Hydrodynamic poles and pole-skipping. Given that the pole-skipping point lies on the line of poles of the two-point function, an intriguing question can arise: which dispersion relation passes through this pole-skipping point? It was shown [12, 13, 19] that the corresponding dispersion relation is the hydrodynamic poles, which vanish at zero wave-vector, i.e., a gapless mode. For instance, the typical example would be the hydrodynamic diffusive mode

$$\omega = \omega_{\text{hy}}(k \rightarrow 0) = -i\mathcal{D}k^2 + \dots, \quad (3)$$

where the full hydrodynamic dispersion relation $\omega_{\text{hy}}(k)$ becomes the diffusive mode in small k limit with the diffusion constant \mathcal{D} . As emphasized in [19], it is a highly non-trivial statement that regardless of the details of the full dispersion relation, the pole-skipping always satisfies the constraint $\omega_{\text{hy}}(k_*) = \omega_*$. Thus, one of the major roles of the pole-skipping is that it can serve as the role of the non-trivial constraint on the “full” hydrodynamic pole $\omega_{\text{hy}}(k)$.

In general, the pole-skipping point associated with the chaotic behavior (2) lies beyond the typical scope of validity of hydrodynamics, i.e., outside the regime where small (ω, k) expansions are applicable. This implies that beyond its role as a constraint, it might be challenging to establish direct physical implications of the pole-skipping point, such as its direct relationship with the diffusion constant since the higher-order correction in k is also important.

Nevertheless, in a series of recent works [19, 34, 37], the potential significance of the pole-skipping on the diffusion constant has been unveiled. Specifically, by utilizing a holographic model with momentum relaxation, it has been demonstrated that a universal lower bound of the longitudinal diffusion constant (e.g., energy diffusion

constant), which is attained in the strong momentum relaxation limit (or at low temperature), can be related to the chaotic pole-skipping point (2) as

$$\omega_* = -iD_e k_*^2 \quad \longrightarrow \quad \frac{D_e \lambda_L}{v_B^2} = 1, \quad (4)$$

where D_e is the energy diffusion constant. The former one implies that (2) passes through the energy diffusive mode in the strong momentum limit, while the latter corresponds to the celebrated universal bound in holography [8, 9]. See also [7, 10, 11, 17, 48–63] for the considerable success of this universal bound.

In essence, pole-skipping served not only as a non-trivial constraint on the full hydrodynamic dispersion relation, but also provides a new approach to capture a universal bound of energy diffusion constant.

The purpose of this manuscript is to further explore the generality of role of the pole-skipping in the energy density two-point function. In particular, we intend to investigate the IR fixed point dependence in (4). It is shown that a universal bound depends on the IR fixed point as $D_e \lambda_L / v_B^2 = z / (2(z - 1))$ where z is the critical dynamical exponent.¹ In other words, the relationship (4) has only been verified for a specific IR fixed point case [19, 34, 37]: $\text{AdS}_2 \times R^2$ fixed point.

In the main context, specifically within the framework of the Gubser-Rocha model, we will explicitly demonstrate that (4) may not hold true beyond the scenario of $\text{AdS}_2 \times R^2$ fixed point.

It is noteworthy that the universal bound of the diffusion constant, expressed as $D_e \lambda_L / v_B^2 = z / (2(z - 1))$, has been verified through an analysis of the IR geometry [11]. In this analysis, the entire left-hand side of the bound can be formulated in terms of the horizon data. This signifies that the evaluation of such a quantity can be straightforwardly accomplished using the IR geometries once the background solution is provided.

However, to investigate the role of pole-skipping as an alternative interpretation of the universal bound, it is essential to solve the equations of motion for fluctuations and compute the corresponding quasi-normal modes. Unlike the background solution, these modes cannot be readily determined, necessitating a model-by-model exploration of gravity theories.

Therefore, for a comprehensive examination of the pole-skipping as an alternative interpretation of the universal bound, it becomes imperative to calculate the quasi-normal mode in scenarios where the IR fixed point does not correspond to the $\text{AdS}_2 \times R^2$ fixed point. The verification of whether (4) holds in such cases is crucial.

¹ The bound is not well defined at $z = 1$ which presents an issue as it corresponds to an irrelevant deformation of the quantum critical state. An independent and distinct analysis is required in this scenario as in [64].

It is also important to note that computing quasi-normal modes involves nontrivial numerical computations rather than relying on analytic IR analysis.

Consequently, for the specific purpose of scrutinizing (4), it suffices to identify a single counterexample where (4) is not satisfied, indicating a situation where the pole-skipping point cannot pass through the (leading) hydrodynamic diffusive mode given by (3).

Furthermore, we also aim to discuss further on the role of pole-skipping as a constraint on the full hydrodynamic dispersion relation $\omega_{\text{hy}}(k)$. In particular, we will show that given two conditions,

$$\omega_{\text{hy}}(k \rightarrow 0) = -iD_e k^2, \quad \omega_{\text{hy}}(k_*) = \omega_*, \quad (5)$$

one may find the effective approximation in strong momentum relaxation limit. See also [44] for the reconstruction of the spectrum of transverse momentum two-point function from pole-skipping using different method.

The manuscript is organized as follows. In Section II, we introduce the Einstein-Maxwell-Dilaton theory coupled to axion fields (EMDA model). Here, we present the thermodynamic quantities, including the energy diffusion constant and quantities related to quantum chaos. In addition, we provide gauge-invariant fluctuation bulk fields convenient for the computation of quasi-normal modes. In Section III we give a review of the Gubser-Rocha model—a specific holographic model of EMDA model. We discuss its thermodynamic properties and energy diffusion bound. The Section IV is dedicated to the computation of quasi-normal modes for the Gubser-Rocha model. We study the pole-skipping phenomena and explore its connection to the bound of energy diffusion constant. Furthermore, we discuss how pole-skipping may contribute to the reconstruction of the full hydrodynamic dispersion relation, particularly in the context of energy diffusion. In Section V, we conclude.

II. PRELIMINARIES

A. Einstein-Maxwell-Dilaton-Axion model

Let us first review the representative holographic model with momentum relaxation in (3+1) dimensions, which is the Einstein-Maxwell-Dilaton-Axion model [65]

$$\begin{aligned} S &= \int d^4x \sqrt{-g} (\mathcal{L}_1 + \mathcal{L}_2), \\ \mathcal{L}_1 &= R - \frac{Z(\phi)}{4} F^2 - \frac{1}{2} (\partial\phi)^2 + V(\phi), \\ \mathcal{L}_2 &= -\frac{Y(\phi)}{2} \sum_{I=x,y} (\partial\psi_I)^2, \end{aligned} \quad (6)$$

where \mathcal{L}_1 consists of two matter fields: the $U(1)$ gauge field with its field strength $F = dA$ together with the dilaton field ϕ . The other matter field, called axion fields ψ ,

is introduced as in \mathcal{L}_2 to consider the momentum relaxation, i.e., in order to obtain finite conductivities.

Next, considering the homogeneous ansatz

$$\begin{aligned} ds^2 &= -D(r)dt^2 + B(r)dr^2 + C(r)(dx^2 + dy^2), \\ A &= A_t(r)dt, \quad \phi = \phi(r), \\ \psi_x &= m x, \quad \psi_y = m y, \end{aligned} \quad (7)$$

where m denotes the strength of momentum relaxation, one can find the thermodynamic quantities evaluated at the black brane horizon r_h as

$$\begin{aligned} T &= \frac{1}{4\pi} \frac{D'}{\sqrt{DB}} \Big|_{r_h}, \quad s = 4\pi C \Big|_{r_h}, \quad \rho = \frac{ZCA'_t}{\sqrt{DB}} \Big|_{r_h}, \\ \kappa &= \frac{4\pi s T Z C}{\rho^2 + k^2 Y Z C} \Big|_{r_h}, \quad c_\rho = 4\pi T C' \Big|_{r_h} \frac{\partial r_h}{\partial T}. \end{aligned} \quad (8)$$

Here T is the Hawking temperature, s entropy density, ρ charge density. The other quantities are that κ is the thermal conductivity in the open circuit condition and c_ρ the specific heat.

The main objective in this manuscript are the energy diffusion constant D_e together with two quantum chaos quantities (λ_L, v_B). They can also be determined by the horizon data as

$$D_e = \frac{\kappa}{c_\rho}, \quad \lambda_L = 2\pi T, \quad v_B^2 = \frac{2\pi T \sqrt{D(r_h)B(r_h)}}{C'(r_h)}. \quad (9)$$

Note that the chaos quantities above for the action (6) are obtained by the near-horizon analysis for pole-skipping in [34], which are also consistent with the one by the shock-wave analysis [56].

B. Fluctuation bulk fields and quasi-normal modes

Next, in order to study the poles in holography, i.e., the quasi-normal modes, we consider the following bulk fluctuations based on the background geometry (7)

$$\begin{aligned} g_{\mu\nu} &\rightarrow g_{\mu\nu} + \delta g_{\mu\nu}, \quad A_\mu \rightarrow A_\mu + \delta A_\mu, \\ \phi &\rightarrow \phi + \delta\phi, \quad \psi_I \rightarrow \psi_I + \delta\psi_I, \end{aligned} \quad (10)$$

where all the fluctuations (collectively labeled as $\delta\mathcal{F}$ below) can be expressed in the Fourier form as

$$\delta\mathcal{F} = \delta\bar{\mathcal{F}}(r) e^{-i\omega t + ikx}. \quad (11)$$

For simplicity, we set the radial gauge as $\delta g_{\mu r} = \delta A_r = 0$.

At the linearized fluctuation equations of motion, we have two decoupled channels: longitudinal or transverse channel. Furthermore, implementing the standard holographic technique [66], one can find the relevant variables (denoted as Z_i below) associated with the diffeomorphism invariance together with the gauge invariance.

These variables are useful for the numerical computations of quasi-normal mode and found to be as follows

for each channels:

1. Longitudinal channel:

$$\begin{aligned} Z_1 &:= \frac{4k}{\omega} \delta \bar{g}_t^x + 2\delta \bar{g}_x^x - \left(2 - \frac{2k^2 D'}{\omega^2 C'}\right) \delta \bar{g}_y^y + \frac{2k^2 D}{\omega^2 C} \delta \bar{g}_t^t, \\ Z_2 &:= k \delta \bar{A}_t + \omega \delta \bar{A}_x - \frac{kC}{C'} A'_t \delta \bar{g}_y^y, \\ Z_3 &:= \delta \bar{\psi}_x + \frac{im}{2k} (\delta \bar{g}_x^x - \delta \bar{g}_y^y), \\ Z_4 &:= \delta \bar{\phi} - \frac{C}{C'} \phi' \delta \bar{g}_y^y. \end{aligned} \quad (12)$$

2. Transverse channel:

$$\begin{aligned} Z_5 &:= k \delta \bar{g}_t^y + \omega \delta \bar{g}_x^y, \\ Z_6 &:= \delta \bar{A}_y, \\ Z_7 &:= \delta \bar{\psi}_y + \frac{im}{k} \delta \bar{g}_x^y. \end{aligned} \quad (13)$$

Subsequently, by solving the fluctuation equations of motion expressed in terms of Z_i , one can construct the source matrix \mathcal{S} , where it is built by collecting the leading coefficients of Z_i near the AdS boundary. Finally, quasi-normal mode can be determined by the values of (ω, k) at which the determinant of \mathcal{S} vanishes [67].

III. GUBSER-ROCHA MODEL

As outlined in the introduction section, one primary purpose of this manuscript is to investigate the IR fixed point dependence in pole-skipping. Recall that, the verification of (4) at the different IR fixed point requires a model-by-model exploration of gravity theories. To do this, we employ the Gubser-Rocha model [68] as an illustrative example, which is a specific model within a broader class of models (6) as

$$Z(\phi) = e^{\frac{\phi}{\sqrt{3}}}, \quad V(\phi) = 6 \cosh \frac{\phi}{\sqrt{3}}, \quad Y(\phi) = 1. \quad (14)$$

This model has been recognized as a effective holographic model for condensed matter systems [65, 69]. In particular, its IR scale invariant point, which falls into the class of the semi-local quantum liquids [70], is responsible for the characteristics of strange metals.² Note that this fixed point is also referred to as the conformal to $\text{AdS}_2 \times R^2$ fixed point which is different from the one examined in prior investigations of pole-skipping [19, 34, 37].

² For instance, see [71–77] for the linear- T resistivity, fermionic spectral function, and Homes's law in high temperature superconductors. See also [78] for its limitation to describe the transport anomalies such as Hall angle.

Another intriguing aspect of the Gubser-Rocha model (14) is that it allows an analytic background solutions as

$$\begin{aligned} D(r) &= \frac{1}{B(r)} = r^2 h(r) g(r), \quad C(r) = r^2 g(r), \\ A_t(r) &= \sqrt{3Q(Q+r_h) \left(1 - \frac{m^2}{2(Q+r_h)^2}\right)} \left(1 - \frac{Q+r_h}{Q+r}\right), \\ \phi(r) &= \frac{1}{\sqrt{3}} \log g(r), \end{aligned} \quad (15)$$

where

$$\begin{aligned} h(r) &= 1 - \frac{m^2}{2(Q+r)^2} - \frac{(Q+r_h)^3}{(Q+r)^3} \left(1 - \frac{m^2}{2(Q+r_h)^2}\right), \\ g(r) &= \left(1 + \frac{Q}{r}\right)^{\frac{3}{2}}. \end{aligned} \quad (16)$$

Last but not least, it is worth noting that exploring pole-skipping together with the quasi-normal mode of Gubser-Rocha model can be considered as a natural extension of previous literature [19, 34, 37] based on the linear-axion model [79]. This is because the Gubser-Rocha model undergoes the phase transition to the linear-axion model when the momentum relaxation is weak [58], as we will elaborate on shortly. In addition, to the best of our knowledge, our work is the first study considering the quasi-normal mode of the Gubser-Rocha model.

In short, in this paper, we choose the Gubser-Rocha model (14) for three main reasons: (I) it features distinct IR fixed points compared to those explored in previous works such as [19, 34, 37]; (II) it allows an analytical background solutions (15)-(16); (III) it can be associated with [19, 34, 37] through a phase transition.

Thermodynamics and energy diffusion bound.

Plugging (15)-(16) into (8), the Hawking temperature T and chemical potential $\mu := A_t(r \rightarrow \infty)$ read as

$$\begin{aligned} T &= \frac{\sqrt{r_h} (6(Q+r_h)^2 - m^2)}{8\pi(Q+r_h)^{3/2}}, \\ \mu &= \sqrt{3Q(Q+r_h) \left(1 - \frac{m^2}{2(Q+r_h)^2}\right)}. \end{aligned} \quad (17)$$

Note that at finite density, there could be two diffusion constants that describe the coupled diffusion of charge and energy [80]. In this manuscript, we focus on the longitudinal channel at zero density in order to exclusively investigate energy diffusive as in [19, 34, 37].

For the neutral case ($\mu = \rho = 0$), one can find two solutions from (17):

$$Q = 0, \quad Q = \frac{m}{\sqrt{2}} - r_h, \quad (18)$$

where another solution $Q = -r_h$ is not allowed due to the thermodynamic instability [58].

The first solution in (18) corresponds to the case with a vanishing dilaton field ϕ , i.e., it is a linear-axion model studied in previous literature [19, 34, 37]. On the other hand, the latter solution has a non-trivial dilaton field profile.

One comment is in order. One can note a distinction in the nature of fixed points between the models in (18), as demonstrated in the analysis of the IR geometry [65]. While both cases share the property of having an infinite critical dynamical exponent, i.e., $z \rightarrow \infty$, there exists a disparity in the hyperscaling violating exponent θ : it approaches zero for the linear-axion model, whereas it diverges for the Gubser-Rocha model. This prompts the question of why the values of bound of energy diffusion constant differ between these models, given their shared critical dynamical exponent.

The discrepancy may arise from the assumption used to derive such a bound, which relies on the vanishing entropy density $s \approx T^{(d-\theta)/z}$ [11]. This assumption is not applicable to the linear-axion model, as it exhibits a residual entropy at low temperatures. Consequently, a separate calculation is required to determine the bound for the linear-axion model. For a more extensive discussion on this matter, we refer to [11].

In order to determine which solution in (18) is the ground state, the following quantity can be useful

$$\Delta G := G|_{Q=0} - G|_{Q=\frac{m}{\sqrt{2}}-r_h}, \quad (19)$$

where G is the grand potential density [81] found as

$$G = -(Q + r_h)^3 - \frac{r_h m^2}{2}. \quad (20)$$

Hereafter, we fix the horizon radius $r_h = 1$ and all the physical quantities are scaled by the temperature T , i.e., $(m/T, \omega/T, k/T, D_e T, \text{etc.})$.

In Fig. 1, we display (19) with respect to m/T and find that $Q = 0$ is the ground state for $m/T < 2\sqrt{2}\pi$, while $Q = \frac{m}{\sqrt{2}} - r_h$ is the one for $m/T > 2\sqrt{2}\pi$. Thus, when the momentum relaxation is weak, the Gubser-Rocha model ($Q \neq 0$) can undergo phase transition to the linear-axion model ($Q = 0$) [58]. The critical phase transition point (m_c/T) can be found analytically as

$$\frac{m_c}{T} = 2\sqrt{2}\pi, \quad (21)$$

which is achieved when $\Delta G = 0$.

Using (9) together with (15)-(16) at zero density, we also find the energy diffusion constant

$$D_e = \begin{cases} \frac{\sqrt{6m^2+16\pi^2 T^2}}{2m^2} & (Q = 0), \\ \frac{4\pi T}{m^2} & (Q = \frac{m}{\sqrt{2}} - r_h), \end{cases} \quad (22)$$

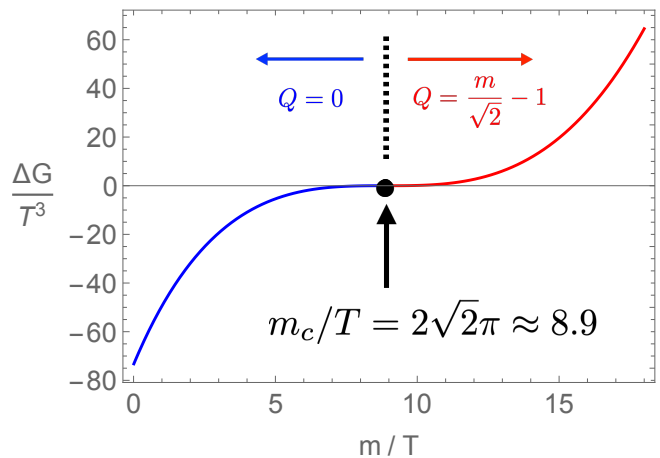


Figure 1. The difference of a grand potential density (19). $Q = 0$ is the ground state for $m/T < 2\sqrt{2}\pi$ and $Q = \frac{m}{\sqrt{2}} - r_h$ is the one for $m/T > 2\sqrt{2}\pi$.

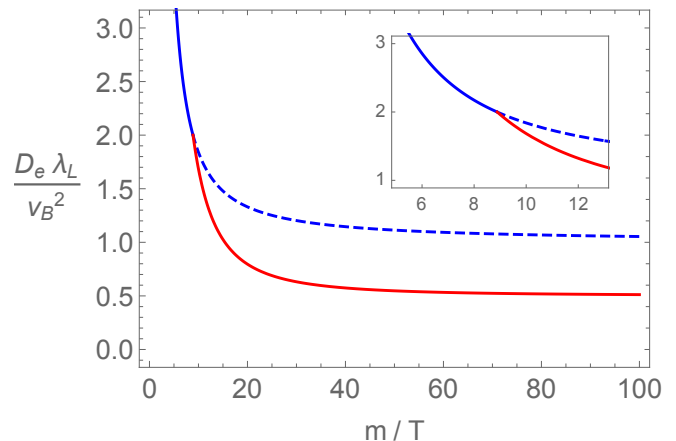


Figure 2. Bound of energy diffusion constant. Solid line represents the result for the ground state where $m_c/T \approx 8.9$. Dashed line after $m > m_c$ is the result of the linear-axion model (i.e., not the ground state). The lower bound $D_e \lambda_L / v_B^2 = 1, 1/2$ for linear-axion model (blue data) and Gubser-Rocha model (red data), respectively.

and butterfly velocity as

$$v_B^2 = \begin{cases} \frac{6\pi T}{4\pi T + \sqrt{6m^2 + 16\pi^2 T^2}} & (Q = 0), \\ \frac{16\pi^2 T^2}{24\pi^2 T^2 + m^2} & (Q = \frac{m}{\sqrt{2}} - r_h). \end{cases} \quad (23)$$

In Fig. 2, we plot the dimensionless energy diffusion constant $D_e \lambda_L / v_B^2$ where it has its lower bound at strong momentum relaxation limit as $D_e \lambda_L / v_B^2 = 1, 1/2$ for linear-axion model (blue data) and Gubser-Rocha model (red data), respectively.

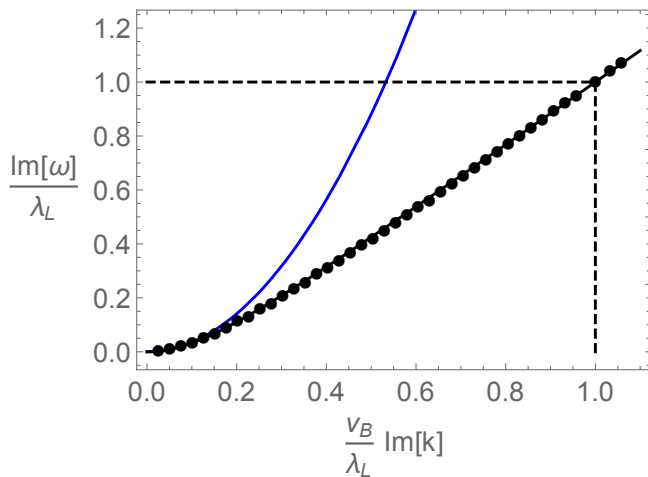


Figure 3. Quasi-normal mode at $m/T = 5$. Dots are numerically obtained quasi-normal mode. The pole-skipping point (2) is denoted by dashed lines. Blue solid line is the diffusive mode (24) and black solid line is (31).

IV. POLE-SKIPPING

Quasi-normal spectrum and pole-skipping. Next, we explore the quasi-normal mode of the longitudinal channel in the Gubser-Rocha model. As introduced in Section II B, we built the source matrix by solving the fluctuation equations of motion from longitudinal channel (12). Consequently, evaluating the determinant of the source matrix, we obtain the quasi-normal mode.

In Fig. 3, we present the representative data of quasi-normal mode at $m/T = 5$ where the linear-axion model is the ground state. Dots are numerically obtained quasi-normal mode where one of the poles corresponds to the pole-skipping point (2). In the small k limit, quasi-normal modes are well approximated by the energy diffusive hydrodynamic mode

$$\omega(k) = -iD_e k^2, \quad (24)$$

which is denoted as the blue solid line in the figure.

As elaborated in the introduction section, it is demonstrated that, in general, the diffusive mode (24) can extrapolate to the pole-skipping point (2) when higher-order corrections in k are taken into account. This is exemplified (by black solid line (31)) in Fig. 3.

However, such higher-order corrections become negligible as we increase the value of m/T . Consequently, the pole-skipping point can pass through (24) [19, 34, 37], which results in a new way of understanding the bound of energy diffusion constant (4).

In Fig. 4, we display the data at $m/T = 100$. The upper panel is for the linear-axion model (i.e., it reproduces the result in [19]), which shows (4).

However, from the lower panel of the figure, we find that the diffusive mode (24) does not pass through the pole-skipping point for the case of the Gubser-Rocha

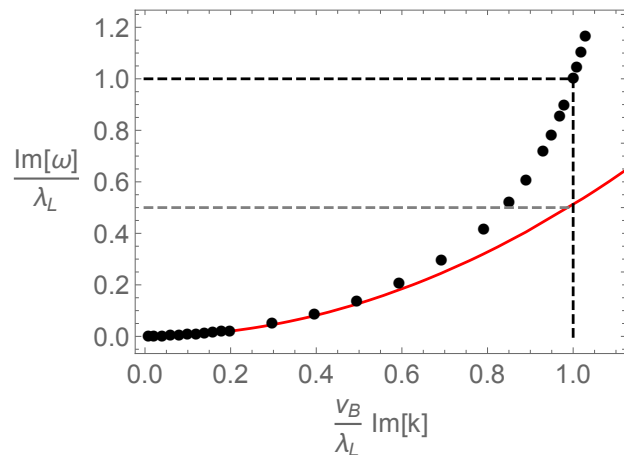
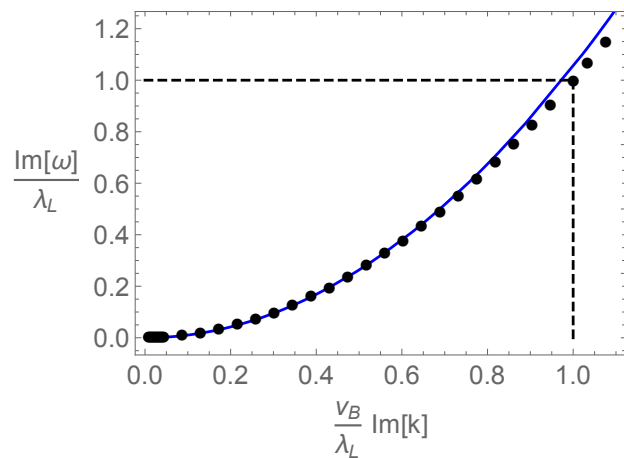


Figure 4. Quasi-normal mode at $m/T = 100$. Upper panel is for the linear-axion model ($Q = 0$), while the lower panel is for Gubser-Rocha model ($Q = \frac{m}{\sqrt{2}} - r_h$). Dots are numerically obtained quasi-normal mode. Black dashed lines indicate the pole-skipping point (2) and solid lines are the diffusive mode (24). Gray dashed line in the lower panel is (25).

model even in the strong momentum relaxation limit. We explore on this point further by some analytic treatment later.

Nevertheless, the diffusion bound of Gubser-Rocha model, $D_e \lambda_L / v_B^2 = 1/2$, can be understood by the fact that the diffusive mode instead passes through $\omega = \omega_*/2$ when $k = k_*$ as indicated as a gray dashed line in Fig. 4, i.e.,

$$\frac{\omega_*}{2} = -iD_e k_*^2 \quad \longrightarrow \quad \frac{D_e \lambda_L}{v_B^2} = \frac{1}{2}. \quad (25)$$

Thus, we argue that for the generic IR fixed point, the pole-skipping argument for the energy diffusion bound (4) should be refined as

$$\tilde{\omega}_* = -iD_e k_*^2 \quad \longrightarrow \quad \frac{D_e \lambda_L}{v_B^2} = \frac{z}{2(z-1)}, \quad (26)$$

where

$$\tilde{\omega}_* := \frac{z}{2(z-1)}\omega_*. \quad (27)$$

In other words, the phenomena where the energy diffusive mode (24) passes through the pole-skipping point (i.e., $\tilde{\omega}_* = \omega_*$) in strong momentum relation limit may only be the case for the specific IR fixed point [19, 34, 37]. It would also be worth noting that equations (26)-(27) are not the result of a mathematical derivation; rather, they are formulated to align with the well-established universal bound.

Reconstruction of quasi-normal spectrum from pole-skipping. In addition to expanding the pole-skipping argument of the energy diffusion bound for generic IR fixed point, we also explore another aspect of the pole-skipping: a constraint on the full hydrodynamic dispersion relation $\omega_{\text{hy}}(k)$ (i.e, quasi-normal modes).

For this purpose, we use the following ansatz for $\omega_{\text{hy}}(k)$

$$\omega_{\text{hy}}(k) = i c_1 \left(\sqrt{c_2 - c_3 k^2} - \sqrt{c_2} \right), \quad (28)$$

where we have three unknown coefficients (c_1, c_2, c_3) .³ Its functional form is motivated by [82] where the linear-axion model at $m = \sqrt{2}r_h$ allows the full analytic (energy diffusive) hydrodynamic dispersion relation. Note that the phase at $m = \sqrt{2}r_h$ is a $\text{SL}(2, \mathbb{R}) \times \text{SL}(2, \mathbb{R})$ invariant point [82] and we find that such a value corresponds to the phase transition point, i.e., $m = m_c \approx 8.9T$ in (21).

More specifically, when $m = m_c$ [82] the coefficients (c_1, c_2, c_3) in (28) are

$$c_1 = \frac{r_h}{2}, \quad c_2 = 1, \quad c_3 = \frac{4}{r_h^2}. \quad (29)$$

The main goal here is to determine (c_1, c_2, c_3) for a generic value of m , relying on two conditions outlined in (5): (I) $\omega_{\text{hy}}(k)$ exhibits the energy diffusive mode (24) at small k ; (II) $\omega_{\text{hy}}(k)$ passes through a pole-skipping point (2). These conditions are consistently observed in all the data presented in Fig. 3-4.

We find that each condition produces specific relationships between coefficients as

$$c_1 = \frac{2\sqrt{c_2}}{c_3} D_e, \quad c_3 = 4 c_2 D_e \left(\frac{D_e}{v_B^2} - \frac{1}{\lambda_L} \right), \quad (30)$$

where c_2 remains undetermined at this level. However, when we plug (30) into (28), the remaining coefficient c_2

is canceled out. Consequently, (28) becomes

$$\omega_{\text{hy}}(k) = \frac{i}{2 \left(\frac{D_e}{v_B^2} - \frac{1}{\lambda_L} \right)} \left[\sqrt{1 - 4D_e \left(\frac{D_e}{v_B^2} - \frac{1}{\lambda_L} \right) k^2} - 1 \right]. \quad (31)$$

It would also be worth noting that the expression (31) (or the ansatz (28)) is not derived from rigorous mathematics but is instead based on assumptions derived from the findings at $m = m_c$ in [82]. As such, (31) can be considered as a heuristically effective fitting. It would be interesting to explore the possibility of a derivation of (31) in near future.

To validate our analysis, we make the plot of (31) as the black solid line in Fig. 3. This shows that (31) is not only well matched with (24) at small k , but also can be a good approximation to the quasi-normal mode beyond the hydrodynamic regime (even around the pole-skipping point). We also check that (31) is also valid for the large strong momentum relaxation case: see Fig. 5. We will discuss further on this figure in the conclusion section.

Two remarks are in order. The hydrodynamic mode we identified, (31), is composed of three physical quantities: (D_e, v_B, λ_L) . This implies that with the use of (31), it may become possible to investigate the ‘‘full’’ (energy diffusive) hydrodynamic gapless mode based on the horizon data (9), i.e., no need to solve the fluctuation equations of motion.

Furthermore, utilizing the expression (31), we can also gain insight into why the energy diffusive mode (24) is not a good approximation for the Gubser-Rocha model, as depicted in Fig. 4. For instance, when we expand (31) in the small k limit, we obtain the following approximate expression:

$$\omega_{\text{hy}}(k) = -iD_e k^2 - iD_e^2 \left(\frac{D_e}{v_B^2} - \frac{1}{\lambda_L} \right) k^4 + \dots \quad (32)$$

Subsequently, one can examine the ratio between the leading and sub-leading terms, which are evaluated at the pole-skipping wave-vector k_* (2) in the strong momentum relaxation limit as:

$$\left(\frac{D_e}{v_B^2} - \frac{1}{\lambda_L} \right) \frac{D_e \lambda_L^2}{v_B^2} \approx \begin{cases} \frac{2\sqrt{2}3\pi}{m/T} + \dots & (Q = 0), \\ -\frac{1}{4} + \dots & \left(Q = \frac{m}{\sqrt{2}} - r_h \right), \end{cases} \quad (33)$$

where \dots denotes $\mathcal{O}(m/T)^{-2}$ corrections.

The first line ($Q = 0$) is the linear-axion model case, which shows that the ratio vanishes at $m/T \gg 1$ limit. While it remains finite for the Gubser-Rocha model (the second line).

This implies that a higher-order correction in k can still be significant for the Gubser-Rocha model (lower panel in Fig. 4), unlike the linear-axion model (upper panel in Fig. 4).

³ Note that c_2 can be factored out, leading to a redefinition of (c_1, c_3) to maintain two remaining unknown coefficients. This is consistent with our findings presented below (30). However, for the sake of generality, we opt to retain all the coefficients in their original form. Also, it is noteworthy that the functional form bears resemblance to the telegraph equation.

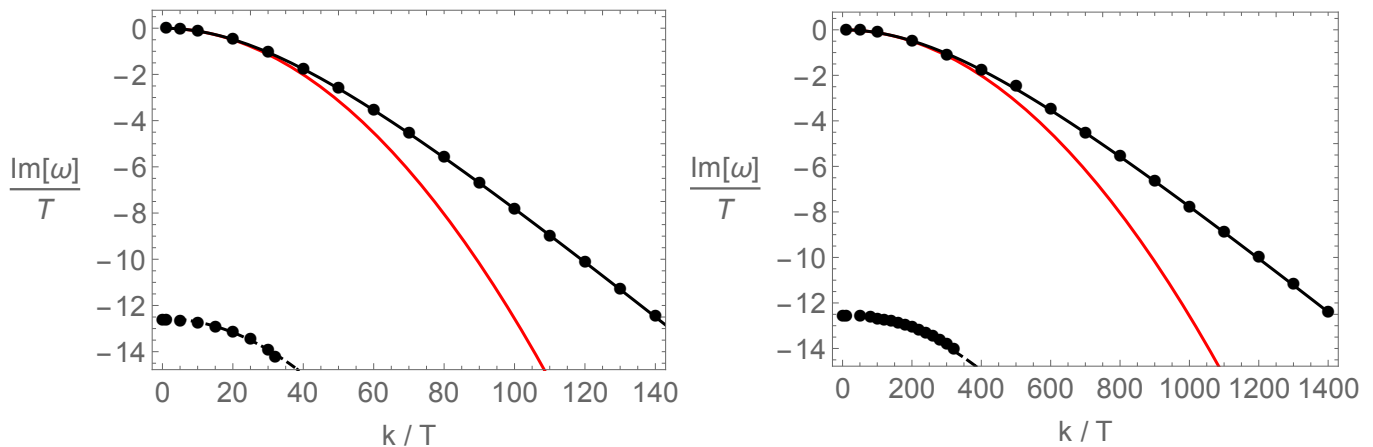


Figure 5. Quasi-normal mode of Gubser-Rocha model at $m/T = 100, 1000$ (left, right). Dots are numerically obtained quasi-normal modes, red solid line is a diffusive mode (24), and black solid line is (31). The dashed line is the fitting curve for the non-hydrodynamic pole (37).

Following the same procedure given by (5), we close this section by proposing a conjecture of the full diffusive hydrodynamic gapless mode with a diffusion constant \mathcal{D} as

$$\omega_{\text{hy}}(k \rightarrow 0) = -i\mathcal{D}k^2, \quad \omega_{\text{hy}}(k_*) = \omega_*, \quad (34)$$

where the pole-skipping point is given by

$$\omega_* := i\omega_{ps}, \quad k_* := ik_{ps}, \quad v_{ps} := \frac{\omega_{ps}}{k_{ps}}. \quad (35)$$

Then, the corresponding $\omega_{\text{hy}}(k)$ can be obtained

$$\omega_{\text{hy}}(k) = \frac{i}{2\left(\frac{\mathcal{D}}{v_{ps}^2} - \frac{1}{\omega_{ps}}\right)} \left[\sqrt{1 - 4\mathcal{D}\left(\frac{\mathcal{D}}{v_{ps}^2} - \frac{1}{\omega_{ps}}\right)k^2} - 1 \right]. \quad (36)$$

One prominent example where this equation can be examined is when translational symmetry is spontaneously broken.

It is instructive to note that our model (14) describes the dual boundary theory when translations are broken explicitly. Furthermore, depending on the type of the symmetry breaking (explicit vs. spontaneous), the longitudinal diffusive dynamics may no longer be governed by energy diffusion; instead, it can become associated with the Goldstone mode [83].

Given that it has been demonstrated in a previous work [34] that a diffusive mode related to the Goldstone mode satisfies (34), it can be of interest to conduct an explicit examination of the applicability of (36) further with the spontaneously broken translations. Moreover, exploring these scenarios with different IR fixed points, as analysed in this paper, can add further relevance to the investigation.

V. CONCLUSIONS

We have studied the pole-skipping phenomena and its relation with quantum chaos. In particular, our study primarily focuses on the IR fixed point dependence on the previously established relationship (4) [19, 34, 37] between pole-skipping and a universal bound of energy diffusion constant.

For this purpose, we choose holographic Gubser-Rocha model, which possesses a semi-locally critical IR fixed point (or the conformal to $\text{AdS}_2 \times R^2$ fixed point) distinct from those examined in previous pole-skipping investigations [19, 34, 37].

Our analysis involves not only an extensive exploration of the thermodynamic properties of the Gubser-Rocha model but also its dispersion relation (i.e., quasi-normal mode), specifically in the longitudinal channel, which is associated with energy diffusion.

We find that the pole-skipping argument for the energy diffusion bound (4) may further be refined as (26)-(27) to accommodate generic fixed points. In other words, we ascertain that the passage of the leading diffusive mode, denoted as $\omega_* = -iD_e k_*^2$, through the pole-skipping point can be contingent upon the nature of the IR fixed point. Given that the verification of (26) demands a thorough investigation of gravity theories on a model-by-model basis, it becomes intriguing to devise methods for assessing (26) (i.e., within quasi-normal mode analysis) in the context of a generic IR fixed point.

In addition to expanding the pole-skipping argument for a diffusion bound concerning generic IR fixed points, we also investigate another aspect of pole-skipping: a constraint on the full hydrodynamic dispersion relation.

Taking into account two conditions (5) where the full hydrodynamic dispersion relation exhibits the energy diffusive mode at small k and passes through a pole-skipping point (2), we have proposed a heuristically effective fit-

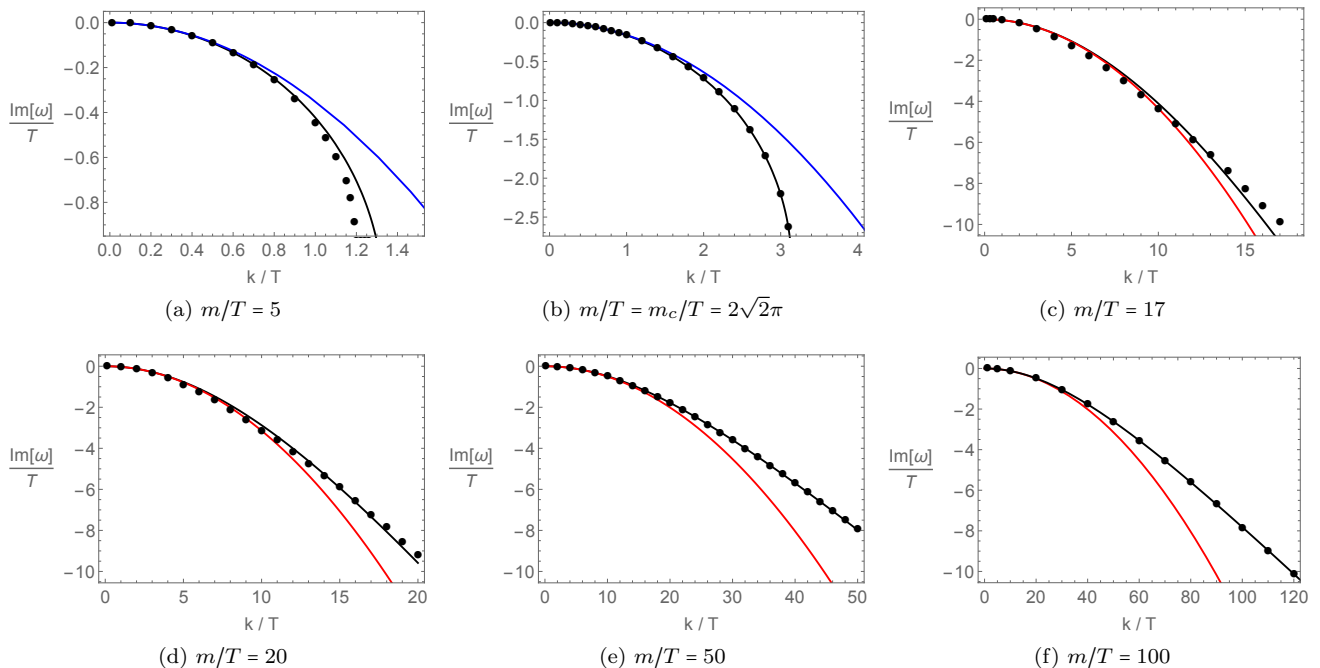


Figure 6. Quasi-normal modes at $m/T = 5, 2\sqrt{2}\pi, 17, 20, 50, 100$. Dots are numerically obtained quasi-normal modes, red (or blue) solid line is a diffusive mode (24), and black solid line is (31). We find that (31) can become a good approximation (even beyond the regime of small ω and k) in the strong momentum relaxation limit, e.g. Fig (e) and (f).

ting (31) for the full energy diffusive hydrodynamic dispersion relation.

This fitting relies on three physical quantities (D_e, v_B, λ_L), all of which can be determined from horizon data. Remarkably, (31) aligns well with the quasi-normal mode even beyond the hydrodynamic regime.

Nevertheless, the effectiveness of our fitting, denoted by (31), is based on $\omega_{\text{hy}}(k_*) = \omega_*$ where k_* is purely imaginary. It is also intriguing to observe that (31) can perform well even in the real k space, as illustrated in Fig. 5, particularly in the regime of strong momentum relaxation.

However, as depicted in Fig. 6, we have confirmed that (31) can deviate from the quasi-normal mode spectrum when we depart from $m = m_c$ as expected. As such, it is essential to note that (31) *assumes* the form of an “effective” heuristic approximation in the limit of *strong* momentum relaxation.⁴ This characterization is presently considered a phenomenological observation, given the elusive nature of its origin.

One intriguing direction for future research inspired by this work involves exploring the “upper” bound of

the energy diffusion constant. Recent conjectures [84–88] suggest a potential upper bound associated with the convergence radius of diffusive hydrodynamic modes. This convergence radius is characterized by the intersection of the gapless diffusive hydrodynamic mode with the first non-hydrodynamic (gapped) mode.

To the best of our knowledge, the upper bound conjecture has only been established for a specific IR fixed point: the linear-axion model. Notably, in such cases, higher-order corrections in k are suppressed in the gapped mode, resulting in nearly constant non-hydrodynamic poles, $\omega_{\text{non-hydro}} = -i4\pi T$.

However, our examination of the Gubser-Rocha model has revealed significant higher-order corrections in both the gapless and gapped modes, as demonstrated in Fig. 5, where we present the non-hydrodynamic poles alongside the fitting curve

$$\omega_{\text{non-hydro}} = -i4\pi T - i\zeta_2 k^2, \quad (37)$$

where ζ_2 is a fitting parameter dependent on m/T . The leading term $-i4\pi T$ aligns with the IR green function analysis in [72].

Given these higher-order corrections, even in the strong momentum relaxation limit, it may not be straightforward to identify the convergence radius for the Gubser-Rocha model, in contrast to the linear-axion model. This intriguing topic requires further investigation, and we leave it as a subject for future research. We hope to elucidate the upper bound of the energy diffusion constant for generic IR fixed points in the near future.

⁴ Nonetheless, even in the strong momentum relation limit, the validity of (31) is subject to limitations. For instance, when $m/T = 50$, the evaluation of ω/T at $k/T = 80$ yields $-i15.3021$ through (31), in contrast to the result of $-i14.9357$ from the numerical quasi-normal mode computation.

ACKNOWLEDGMENTS

We would like to thank Daniel Areán, Yongjun Ahn, Kyoung-Bum Huh, Viktor Jahnke, Juan F. Pedraza for valuable discussions and correspondence. H.-S Jeong acknowledges the support of the Spanish MINECO “Cen-

tro de Excelencia Severo Ochoa” Programme under grant SEV-2012-0249. This work is supported through the grants CEX2020-001007-S and PID2021-123017NB-I00, funded by MCIN/AEI/10.13039/501100011033 and by ERDF A way of making Europe.

-
- [1] A. I. Larkin and Y. N. Ovchinnikov, *JETP* **28**, 6 (1969), 1200.
- [2] J. Maldacena, S. H. Shenker, and D. Stanford, *JHEP* **08**, 106 (2016), arXiv:1503.01409 [hep-th].
- [3] E. Ott, Cambridge University Press (2002), 10.1017/CBO9780511803260.
- [4] P. Gaspard, Cambridge University Press (1998), 10.1017/CBO9780511628856.
- [5] Y. Gu, X.-L. Qi, and D. Stanford, *JHEP* **05**, 125 (2017), arXiv:1609.07832 [hep-th].
- [6] R. A. Davison, W. Fu, A. Georges, Y. Gu, K. Jensen, and S. Sachdev, *Phys. Rev. B* **95**, 155131 (2017), arXiv:1612.00849 [cond-mat.str-el].
- [7] A. A. Patel and S. Sachdev, *Proc. Nat. Acad. Sci.* **114**, 1844 (2017), arXiv:1611.00003 [cond-mat.str-el].
- [8] M. Blake, *Phys. Rev. Lett.* **117**, 091601 (2016), arXiv:1603.08510 [hep-th].
- [9] M. Blake, *Phys. Rev.* **D94**, 086014 (2016), arXiv:1604.01754 [hep-th].
- [10] M. Blake and A. Donos, *JHEP* **02**, 013 (2017), arXiv:1611.09380 [hep-th].
- [11] M. Blake, R. A. Davison, and S. Sachdev, *Phys. Rev. D* **96**, 106008 (2017), arXiv:1705.07896 [hep-th].
- [12] S. Grozdanov, K. Schalm, and V. Scopelliti, *Phys. Rev. Lett.* **120**, 231601 (2018), arXiv:1710.00921 [hep-th].
- [13] M. Blake, H. Lee, and H. Liu, *JHEP* **10**, 127 (2018), arXiv:1801.00010 [hep-th].
- [14] S. Grozdanov, K. Schalm, and V. Scopelliti, *Phys. Rev. E* **99**, 012206 (2019), arXiv:1804.09182 [hep-th].
- [15] A. Lucas, (2017), arXiv:1710.01005 [hep-th].
- [16] T. Hartman, S. A. Hartnoll, and R. Mahajan, *Phys. Rev. Lett.* **119**, 141601 (2017), arXiv:1706.00019 [hep-th].
- [17] R. A. Davison, S. A. Gentle, and B. Gout eraux, *Phys. Rev. Lett.* **123**, 141601 (2019), arXiv:1808.05659 [hep-th].
- [18] F. M. Haehl and M. Rozali, *JHEP* **10**, 118 (2018), arXiv:1808.02898 [hep-th].
- [19] M. Blake, R. A. Davison, S. Grozdanov, and H. Liu, *JHEP* **10**, 035 (2018), arXiv:1809.01169 [hep-th].
- [20] S. Grozdanov, P. K. Kovtun, A. O. Starinets, and P. Tadi c, *JHEP* **11**, 097 (2019), arXiv:1904.12862 [hep-th].
- [21] M. Blake, R. A. Davison, and D. Vegh, *JHEP* **01**, 077 (2020), arXiv:1904.12883 [hep-th].
- [22] M. Natsuume and T. Okamura, *JHEP* **12**, 139 (2019), arXiv:1905.12015 [hep-th].
- [23] M. Natsuume and T. Okamura, *PTEP* **2020**, 013B07 (2020), arXiv:1905.12014 [hep-th].
- [24] M. Natsuume and T. Okamura, *Phys. Rev. D* **100**, 126012 (2019), arXiv:1909.09168 [hep-th].
- [25] N. Ceplak, K. Ramdial, and D. Vegh, *JHEP* **07**, 203 (2020), arXiv:1910.02975 [hep-th].
- [26] Y. Ahn, V. Jahnke, H.-S. Jeong, and K.-Y. Kim, *JHEP* **10**, 257 (2019), arXiv:1907.08030 [hep-th].
- [27] Y. Ahn, V. Jahnke, H.-S. Jeong, K.-Y. Kim, K.-S. Lee, and M. Nishida, *JHEP* **09**, 111 (2020), arXiv:2006.00974 [hep-th].
- [28] N. Abbasi and S. Tahery, *JHEP* **10**, 076 (2020), arXiv:2007.10024 [hep-th].
- [29] Y. Liu and A. Raju, *JHEP* **12**, 027 (2020), arXiv:2005.08508 [hep-th].
- [30] D. M. Ramirez, *JHEP* **12**, 006 (2021), arXiv:2009.00500 [hep-th].
- [31] Y. Ahn, V. Jahnke, H.-S. Jeong, K.-Y. Kim, K.-S. Lee, and M. Nishida, *JHEP* **03**, 175 (2021), arXiv:2010.16166 [hep-th].
- [32] M. Natsuume and T. Okamura, *Phys. Rev. D* **103**, 066017 (2021), arXiv:2011.10093 [hep-th].
- [33] N. Ceplak and D. Vegh, *Phys. Rev. D* **103**, 106009 (2021), arXiv:2101.01490 [hep-th].
- [34] H.-S. Jeong, K.-Y. Kim, and Y.-W. Sun, *JHEP* **07**, 105 (2021), arXiv:2104.13084 [hep-th].
- [35] M. Natsuume and T. Okamura, *Phys. Rev. D* **104**, 126007 (2021), arXiv:2108.07832 [quant-ph].
- [36] M. Blake and R. A. Davison, *JHEP* **01**, 013 (2022), arXiv:2111.11093 [hep-th].
- [37] H.-S. Jeong, K.-Y. Kim, and Y.-W. Sun, *JHEP* **07**, 065 (2022), arXiv:2203.02642 [hep-th].
- [38] D. Wang and Z.-Y. Wang, *Phys. Rev. Lett.* **129**, 231603 (2022), arXiv:2208.01047 [hep-th].
- [39] M. A. G. Amano, M. Blake, C. Cartwright, M. Kaminski, and A. P. Thompson, *JHEP* **02**, 253 (2023), arXiv:2211.00016 [hep-th].
- [40] H. Yuan, X.-H. Ge, K.-Y. Kim, C.-W. Ji, and Y. Ahn, *JHEP* **08**, 157 (2023), arXiv:2303.04801 [hep-th].
- [41] S. Grozdanov and M. Vrbica, (2023), arXiv:2303.15921 [hep-th].
- [42] M. Natsuume and T. Okamura, *Phys. Rev. D* **108**, 046012 (2023), arXiv:2306.03930 [hep-th].
- [43] S. Ning, D. Wang, and Z.-Y. Wang, (2023), arXiv:2308.08191 [hep-th].
- [44] S. Grozdanov, T. Lemut, and J. F. Pedraza, (2023), arXiv:2308.01371 [hep-th].
- [45] H.-S. Jeong, C.-W. Ji, and K.-Y. Kim, *JHEP* **08**, 139 (2023), arXiv:2306.14805 [hep-th].
- [46] M. Natsuume and T. Okamura, (2023), arXiv:2307.11178 [hep-th].
- [47] N. Abbasi and K. Landsteiner, (2023), arXiv:2307.16716 [hep-th].
- [48] A. Lucas, *Phys. Rev. Lett.* **122**, 216601 (2019), arXiv:1809.07769 [cond-mat.str-el].
- [49] Y. Gu, A. Lucas, and X.-L. Qi, *JHEP* **09**, 120 (2017), arXiv:1708.00871 [hep-th].
- [50] Y. Ling and Z.-Y. Xian, *JHEP* **09**, 003 (2017), arXiv:1707.02843 [hep-th].

- [51] Y. Gu, A. Lucas, and X.-L. Qi, *SciPost Phys.* **2**, 018 (2017), [arXiv:1702.08462 \[hep-th\]](#).
- [52] S.-F. Wu, B. Wang, X.-H. Ge, and Y. Tian, *Phys. Rev. D* **97**, 106018 (2018), [arXiv:1702.08803 \[hep-th\]](#).
- [53] W. Li, S. Lin, and J. Mei, *Phys. Rev. D* **100**, 046012 (2019), [arXiv:1905.07684 \[hep-th\]](#).
- [54] X.-H. Ge, S.-J. Sin, Y. Tian, S.-F. Wu, and S.-Y. Wu, *JHEP* **01**, 068 (2018), [arXiv:1712.00705 \[hep-th\]](#).
- [55] W.-J. Li, P. Liu, and J.-P. Wu, *JHEP* **04**, 115 (2018), [arXiv:1710.07896 \[hep-th\]](#).
- [56] H.-S. Jeong, Y. Ahn, D. Ahn, C. Niu, W.-J. Li, and K.-Y. Kim, *JHEP* **01**, 140 (2018), [arXiv:1708.08822 \[hep-th\]](#).
- [57] M. Baggioli and W.-J. Li, *JHEP* **07**, 055 (2017), [arXiv:1705.01766 \[hep-th\]](#).
- [58] K.-Y. Kim and C. Niu, *JHEP* **06**, 030 (2017), [arXiv:1704.00947 \[hep-th\]](#).
- [59] I. L. Aleiner, L. Faoro, and L. B. Ioffe, (2016), [1609.01251](#).
- [60] A. A. Patel, D. Chowdhury, S. Sachdev, and B. Swingle, *Phys. Rev. X* **7**, 031047 (2017), [arXiv:1703.07353 \[cond-mat.str-el\]](#).
- [61] A. Bohrdt, C. B. Mendl, M. Endres, and M. Knap, *New J. Phys.* **19**, 063001 (2017), [arXiv:1612.02434 \[cond-mat.quant-gas\]](#).
- [62] Y. Werman, S. A. Kivelson, and E. Berg, (2017), [arXiv:1705.07895 \[cond-mat.str-el\]](#).
- [63] X. Chen, R. M. Nandkishore, and A. Lucas, *Phys. Rev. B* **101**, 064307 (2020), [arXiv:1912.02190 \[cond-mat.stat-mech\]](#).
- [64] R. A. Davison, S. A. Gentle, and B. Goutéraux, *Phys. Rev. D* **100**, 086020 (2019), [arXiv:1812.11060 \[hep-th\]](#).
- [65] B. Goutéraux, *JHEP* **1404**, 181 (2014), [arXiv:1401.5436 \[hep-th\]](#).
- [66] P. K. Kovtun and A. O. Starinets, *Phys. Rev. D* **72**, 086009 (2005), [arXiv:hep-th/0506184 \[hep-th\]](#).
- [67] M. Kaminski, K. Landsteiner, J. Mas, J. P. Shock, and J. Tarrío, *JHEP* **1002**, 021 (2010), [arXiv:0911.3610 \[hep-th\]](#).
- [68] S. S. Gubser and F. D. Rocha, *Phys. Rev. D* **81**, 046001 (2010), [arXiv:0911.2898 \[hep-th\]](#).
- [69] C. Charmousis, B. Goutéraux, B. Kim, E. Kiritsis, and R. Meyer, *JHEP* **1011**, 151 (2010), [arXiv:1005.4690 \[hep-th\]](#).
- [70] N. Iqbal, H. Liu, and M. Mezei, *JHEP* **04**, 086 (2012), [arXiv:1105.4621 \[hep-th\]](#).
- [71] R. A. Davison, K. Schalm, and J. Zaanen, *Phys. Rev. B* **89**, 245116 (2014), [arXiv:1311.2451 \[hep-th\]](#).
- [72] R. J. Anantua, S. A. Hartnoll, V. L. Martin, and D. M. Ramirez, *JHEP* **1303**, 104 (2013), [arXiv:1210.1590 \[hep-th\]](#).
- [73] H.-S. Jeong, K.-Y. Kim, and C. Niu, *JHEP* **10**, 191 (2018), [arXiv:1806.07739 \[hep-th\]](#).
- [74] Y. Ahn, H.-S. Jeong, D. Ahn, and K.-Y. Kim, *JHEP* **04**, 153 (2020), [arXiv:1907.12168 \[hep-th\]](#).
- [75] H.-S. Jeong, K.-Y. Kim, Y. Seo, S.-J. Sin, and S.-Y. Wu, *Phys. Rev. D* **102**, 026017 (2020), [arXiv:1910.11034 \[hep-th\]](#).
- [76] H.-S. Jeong and K.-Y. Kim, *JHEP* **03**, 060 (2022), [arXiv:2112.01153 \[hep-th\]](#).
- [77] F. Balm *et al.*, (2022), [arXiv:2211.05492 \[cond-mat.str-el\]](#).
- [78] Y. Ahn, M. Baggioli, H.-S. Jeong, and K.-Y. Kim, (2023), [arXiv:2307.04433 \[cond-mat.str-el\]](#).
- [79] T. Andrade and B. Withers, *JHEP* **1405**, 101 (2014), [arXiv:1311.5157 \[hep-th\]](#).
- [80] S. A. Hartnoll, *Nature Phys.* **11**, 54 (2015), [arXiv:1405.3651 \[cond-mat.str-el\]](#).
- [81] M. M. Caldarelli, A. Christodoulou, I. Papadimitriou, and K. Skenderis, *JHEP* **04**, 001 (2017), [arXiv:1612.07214 \[hep-th\]](#).
- [82] R. A. Davison and B. Goutéraux, (2014), [arXiv:1411.1062 \[hep-th\]](#).
- [83] M. Baggioli, K.-Y. Kim, L. Li, and W.-J. Li, *Sci. China Phys. Mech. Astron.* **64**, 270001 (2021), [arXiv:2101.01892 \[hep-th\]](#).
- [84] D. Arean, R. A. Davison, B. Goutéraux, and K. Suzuki, *Phys. Rev. X* **11**, 031024 (2021), [arXiv:2011.12301 \[hep-th\]](#).
- [85] N. Wu, M. Baggioli, and W.-J. Li, *JHEP* **05**, 014 (2021), [arXiv:2102.05810 \[hep-th\]](#).
- [86] H.-S. Jeong, K.-Y. Kim, and Y.-W. Sun, *JHEP* **02**, 006 (2022), [arXiv:2105.03882 \[hep-th\]](#).
- [87] K.-B. Huh, H.-S. Jeong, K.-Y. Kim, and Y.-W. Sun, *JHEP* **07**, 013 (2022), [arXiv:2111.07515 \[hep-th\]](#).
- [88] Y. Liu and X.-M. Wu, *JHEP* **01**, 155 (2022), [arXiv:2111.07770 \[hep-th\]](#).